Power Control of Resonant Converter MPPT by Pulse Density Modulation

Akif Karafil[1], Harun Ozbay[2], and Selim Oncu[3]

[1,2]Bilecik Seyh Edebali University, Bilecik, Turkey
akif.karafil@bilecik.edu.tr, harun.ozbay@bilecik.edu.tr
[3]Karabuk University, Karabuk, Turkey
soncu@karabuk.edu.tr

Abstract

This paper presents the simulation of series resonant converter system with proposed 32 pulse density modulation (PDM) patterns which transfer the electrical energy obtained from PV panels to load with high power density. Maximum power point tracking (MPPT) is achieved by deleting some control pulses. Therefore, zero current switching (ZCS) is achieved at 100 kHz resonant frequency. The average output power changes of series resonant converter are given according to the proposed 32 PDM patterns. Both the MPPT algorithm and the high frequency series resonant converter are controlled by TMS320F28335 DSP. In the 600 W PV system, soft switching condition is achieved by using the proposed 32 PDM technique.

1. Introduction

Photovoltaic systems have gained importance since they convert the solar energy into electrical energy directly, they work silently without giving harm to the environment and they are fast, reliable and have easy set-up. However, the efficiency of the PV panels is very low. Moreover, the output power of the panels varies continuously because of the changing environmental factors. Therefore, MPPT dc-dc converters are used to have the maximum output power of PV panels [1-3].

Many control methods such as frequency control, pulse width modulation (PWM), phase-shift control and duty control are used to control the dc-dc converters. However, these control methods result in an increase of switching losses since hard switching is achieved in all these methods. Switching losses occur when either the current passing through the power switch during the switching or the voltage of switch ends is not zero. Therefore, electromagnetic interferences (EMI) also increase due to high current and voltage spikes occurring during the switching. As a result, operating frequency is limited, efficiency is decreased and the switches are forced due to high switching losses [4-7].

In this study, a series resonant converter MPPT is operated in order to avoid the hard switching conditions and EMI problems occurring in the traditional PWM switched MPPT and to increase the limited operating frequency. The system is operated at higher frequencies compared to PWM controlled converters by providing soft switching conditions. As a result of high operating frequencies, the component sizes and therefore the costs can be reduced. Moreover, PDM technique is more convenient to track the maximum power point at fixed operating frequency for control methods used with resonant converters since the power generated by the PV panels is not same throughout the day. Therefore, it is required for resonant converter systems to operate at frequencies different from the operating frequency. In this study a series resonant converter MPPT circuit is controlled by phase locked loop (PLL) and PDM is simulated in order to have a maximum power point tracking by achieving the soft switching conditions at each power point of 600 W PV system. Therefore, an MPPT circuit operating at soft switching conditions and fixed operating frequency are achieved. The operating frequency of the designed system is 100 kHz and Perturb & Observe (P&O) algorithm is chosen as the MPPT algorithm. P&O algorithm is controlled with a TMS320F28335 DSP.

This paper is organized as follows: Section 2 presents the system design and analysis. This section includes the design of series resonant converter, the analyzed PDM control strategy and power control with PDM. In section 3, the principle of P&O MPPT is presented. Section 4 gives information about the PSIM simulation of the system and analyses results. Finally, some conclusions are drawn in the conclusion part.

2. System Design and Analysis

Today's electronic circuits are expected to be light, small and with high efficiency. PWM technique is generally used in dc-dc converter control. However, the switching losses of PWM controller converters are very high. High switching losses limit dc-dc converter operating frequency, reduce the efficiency and may damage power switches. To overcome these drawbacks, resonant converters are used. Resonant converter is a dc-dc or dc-ac converter obtained by adding the resonant circuit to PWM switching power converter [8-10]. Square wave current is obtained in the inverter output when the power switches of the inverter circuit are switched in a sequence. Sinusoidal load current/voltage wave form is obtained from square wave voltage produced by inductor (L) and capacitor (C) components (resonant circuit). Sinusoidal voltage is rectified by rectifier circuit and transferred to the output to have dc voltage. Series resonant converter circuit is obtained by adding the L_r and C_r components to the converter circuit in series. Resonant frequency (f_r), an important parameter in the control of the circuit, is calculated by the following equation [11, 12].

$$f_r = \frac{1}{2\pi\sqrt{L_r C_r}} \tag{1}$$

A full bridge converter consists of a dc voltage source and four MOSFET power switches. $+V_d$ dc input voltage is obtained in load ends when S_1 and S_4 switches are turn on simultaneously. On the other hand, the voltage in the load ends

is negative and has $-V_d$ value when S_2 and S_3 switches are turn on simultaneously. The circuit configuration of the system and the operating modes are shown in Figure 1 and 2, respectively.

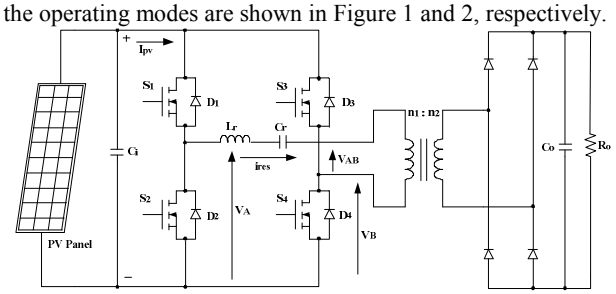

Fig. 1. The circuit configuration of the system

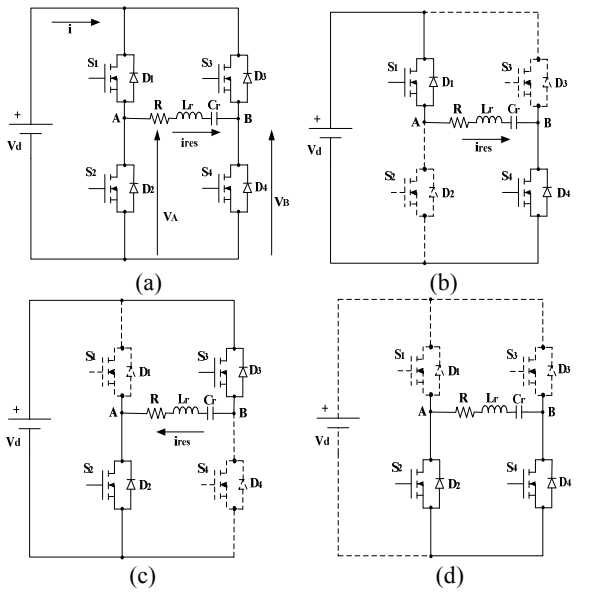

Fig. 2. The operating modes of the simplified circuit: (a) the equivalent circuit (b) Mode I, (c) Mode II and (d) Mode III

S_1 and S_4 switches are turn on in Mode I while S_2 and S_3 switches are turn on in Mode II. The output voltage of the inverter (V_{AB}) is zero in Mode III. The current passing through D_4 diode when S_2 switch is turn on and the current passing through D_2 diode when S_4 switch is turn on are in damped oscillation form. The switching modes and the positions are shown in Table 1.

Table 1. Operating modes

Switching Modes	Off	On
Mode I	S_2 and S_3	S_1 and S_4
Mode II	S_1 and S_4	S_2 and S_3
Mode III	S_1 and S_3	S_2 and D_4 S_4 and D_2

While the output voltage of the inverter is $V_{AB} = +V_d$ (Fig. 2.b) in Mode I, it is as $V_{AB} = -V_d$ (Fig. 2.c) in Mode II. The output voltage of the inverter is $V_{AB}=0$ (Fig. 2.d) in Mode III when the load is disconnected from the source [4, 13-15].

2.1. Analysis of PDM Control Strategy

PDM is among the most suitable control techniques for resonant topologies [16]. PDM is a command sequence. Power control is provided by deleting some of the on pulses in accordance with the command sequences without making any change in the turn on duration of the switch. Power decreases as the number of the deleted pulses increases. The PDM control principle is given in Figure 3.

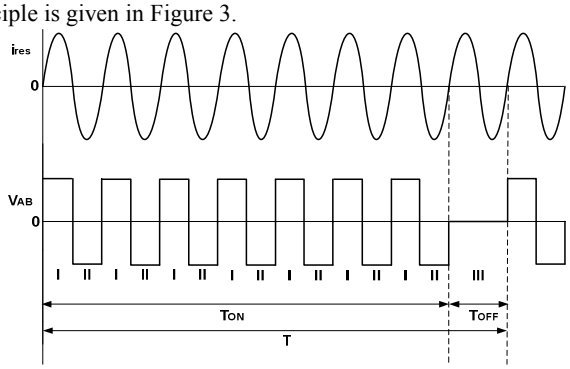

Fig. 3. The basis of PDM control

As seen in the figure, until the seventh resonant cycle square wave voltage (Mode I and II operating) is applied as V_d value. In the 8th cycle on pulse is deleted and zero voltage (Mode III operating) is applied to the inverter. The output voltage of the inverter is in periodic wave form in the eighth resonant cycle. The average output power is 28/32 when compared to the full power operating. That is, the output power of the inverter is controlled by adjusting the pulse density of the square wave voltage.

Turn on and turn off durations of the switches are calculated by the following equation.

$$T = NT_r = T_{on} + T_{off}, T_{on} = N_1 T_r, T_{off} = N_2 T_r, D = \frac{T_{on}}{T} \quad (2)$$

Where; N is the total resonant cycle, N_1 is normal resonant cycle number, N_2 is the controlled (deleted pulse) resonant cycle number.

The following equations are obtained when examining the mathematical analysis of the full bridge series RLC resonant circuit shown in Fig. 2.a.

$$L_r \frac{di_{res}}{dt} + \frac{1}{C_r}\int i_{res}dt + Ri_{res} = V_d(t) \quad (3)$$

$$\tau = \frac{2L_r}{R} = \frac{2Q}{\omega_r} \quad (4)$$

Where, τ is time constant, Q is the quality factor of the series resonant circuit and ω_r is angular resonant frequency.

The following equation is obtained when the $V_d(t)$ principle component is written using Fourier analysis.

$$V_d(t) = \frac{4V_d}{\pi} sin(\omega_r t) \quad (5)$$

The following equation is obtained when the general solution of the equation is written.

$$i_{res}(t)=\left[A\cos(\omega_r t)+B\sin(\omega_r t)\right]e^{-\frac{R}{2L_r}t}+\frac{4V_d}{\pi R}\sin(\omega_r t) \quad (6)$$

When the initial conditions are considered, the resonant current is as follows:

$$i_{res}(t)=\frac{4V_d}{\pi R}\left(1-e^{-\frac{R}{2L_r}t}\right)\sin(\omega_r t) \quad (7)$$

Figure 4 shows the resonant current (i_{res}) and the envelope of the resonant current (i_E). When the resonant current is written at this condition, the following equations are obtained.

$$i_{res}(t)=i_E(t)\sin\omega_r t, \quad (8)$$

$$i_E(t)=A(1-e^{-\frac{t}{\tau}})+B, \qquad 0<t<T_{on}, \quad (9)$$

$$i_E(t)=Ce^{-\frac{t-T_{on}}{\tau}}, \qquad T_{on}<t<T \quad (10)$$

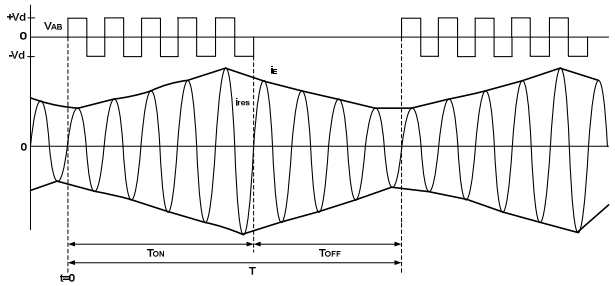

Fig. 4. PDM current wave form

When the i_E current is rewritten using the A, B and C coefficients, the following equations are obtained:

$$i_E(t)=I(1-e^{-\frac{t}{\tau}})+I_{min}e^{-\frac{t}{\tau}}, \qquad 0<t<T_{on}, \quad (11)$$

$$i_E(t)=i_E(T_{on})e^{-\frac{t-T_{on}}{\tau}}, \qquad T_{on}<t<T \quad (12)$$

The average output power is obtained by the following equations:

$$P=\frac{1}{T}\int_0^T V_{AB}(t)i_{res}(t)dt, \quad (13)$$

$$P=P_{max}\left[\frac{T_{on}}{T}+\frac{\tau}{T}\left(\frac{1-e^{-\frac{T_{on}}{\tau}}}{1-e^{-\frac{T}{\tau}}}\right)\left(e^{-\frac{T_{on}}{\tau}}-e^{-\frac{T}{\tau}}\right)\right] \quad (14)$$

If PDM period ($T=NT_r$) is smaller than the time constant ($T<<\tau$), the amplitude of the resonant current is proportional to the pulse density. Therefore, when the relationship between the output power and the pulse density is written, the following equation is obtained:

$$\lim_{\tau\to\infty} P=P_{max}D^2 \quad (15)$$

If PDM period ($T=NT_r$) is bigger than the time constant ($T>>\tau$), the output power is [4, 13]:

$$\lim_{\tau\to 0} P=P_{max}D \quad (16)$$

2.2. PDM and PLL Control Basics

The block diagram of the PDM control circuit designed with PLL is shown in Figure 5. The control circuit consists of two parts. The first part is the PLL circuit where resonant current (i_{res}) and the inverter output voltage (V_{AB}) phase are locked. As a result, zero transition points are detected at resonant frequency and the soft switching conditions are achieved. On the other hand, PLL circuit consists of three parts. These are as follows: phase detector, low pass filter and voltage controlled oscillator (VCO). In the last part of the PLL circuit VCO output signal is compared with a triangular signal comparator and PWM pulses are obtained. The obtained PWM pulses are sent to frequency divider and parallel input serial output (PISO) register of the PDM logic circuit, which is the second part of the control circuit. The parallel inputs required for the shift register are the proposed 32 PDM pulses and obtained from the digital output of the DSP.

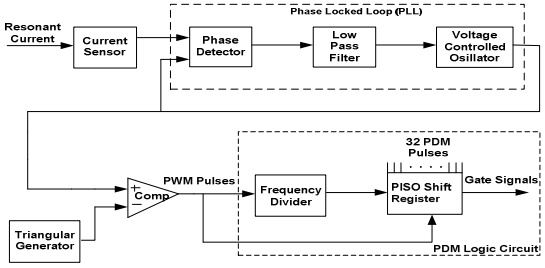

Fig. 5. The block diagram of the designed PDM control circuit

A table is prepared to choose the proposed PDM patterns for the PDM control unit in order to generate switch driving signals. Figure 6 shows the proposed PDM switching forms for N=32. Table consists of 0 and 1 bites.

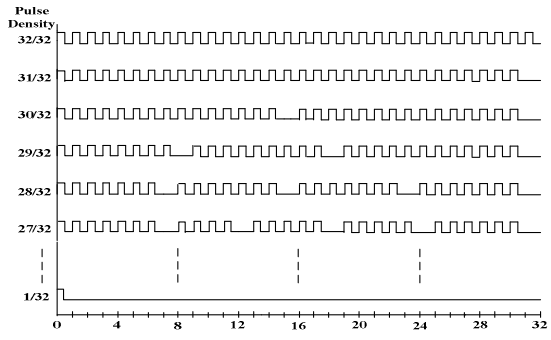

Fig. 6. The proposed 32 PDM patterns

In the table, N represents the lines and 2*N represents the columns. On the other hand, 32 lines represent the different levels for PDM (N=1/32…32/32). The columns represent the 32 resonant cycles generated to control the inverter switches. The duration of each cycle is equal to the resonant duration ($T=NT_r$).

3. MPPT with PDM Control

MPPT is completely an electronic system tracking the maximum power by tracking the maximum power of PV panel. In MPPT algorithm, input voltage and current are tracked continuously and simultaneously, the changes are calculated and the necessary steps are followed to obtain the maximum power point (MPP) [17].

In this study, P&O method, which is one of the most used methods, was preferred due to its simplicity and high efficiency. In P&O method, PV panel power is measured when the change is applied to the control parameter and it is compared to the previous measured power. The flow chart of the PDM controlled P&O MPPT algorithm is shown in Figure 7.

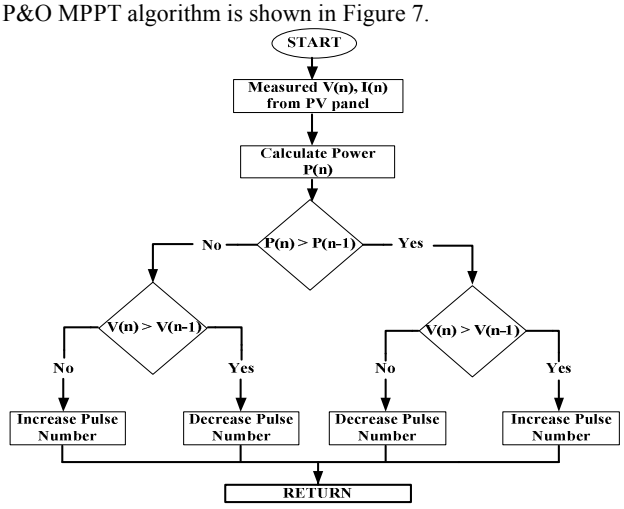

Fig. 7. The flow chart of PDM controlled P&O MPPT algorithm

If the power and voltage increases, the change is applied in the same direction in the next step. Therefore, PDM switching signal also increases. If the power decreases and the voltage increases or the power increases and the voltage decreases, then PDM signal decreases. On the contrary, if both the power and the voltage decrease, PDM signal increases. Figure 8 shows the resonant converter MPPT system.

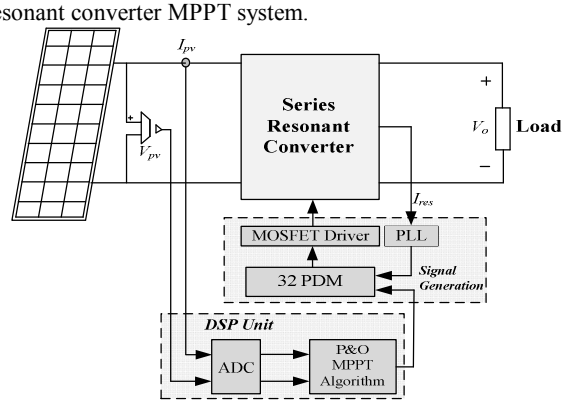

Fig. 8. The block schema of the resonant converter MPPT system

Figure 8 shows the overall block diagram of the proposed system consisting of the PV generator, the P&O MPPT control algorithm, PLL, PDM, resonant converter and the DSP unit. In the designed system, the generated power is calculated with DSP by using the measured PV voltage and current. DSP provides the control of the system by deleting some of the control pulses of the resonant converter according to the P&O algorithm. Therefore, PV panels are operated at their maximum power.

4. PSIM Simulation Results

The proposed 32 PDM controlled series resonant converter MPPT circuit simulated at PSIM is shown in Figure 9.

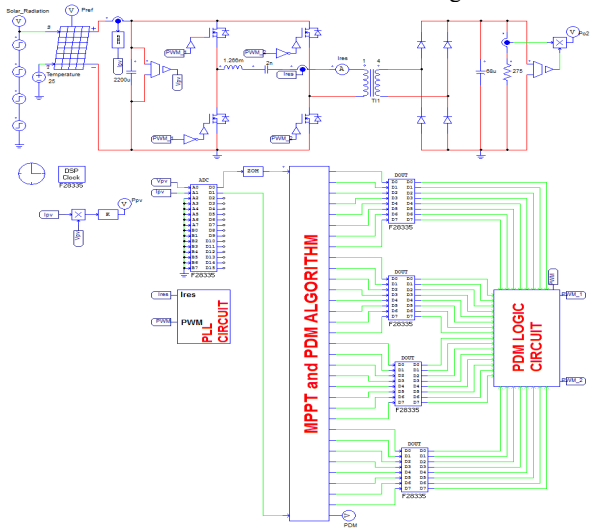

Fig. 9. The proposed 32 PDM controlled series resonant converter MPPT circuit

When the maximum PDM length N=32 ($T=32T_r$) is chosen, pulse density D will change from 1/32 to 32/32. While the minimum power is obtained at 1/32 condition, maximum power is obtained at 32/32 condition. The pulse density changes depending on the power amount obtained from PV panels. In this study, P&O MPPT algorithm and 32 cycled PDM table are written into the simplified C block. The average output power of the full bridge series resonant converter circuit simulated and calculated according to the PDM signals is shown in Figure 10.

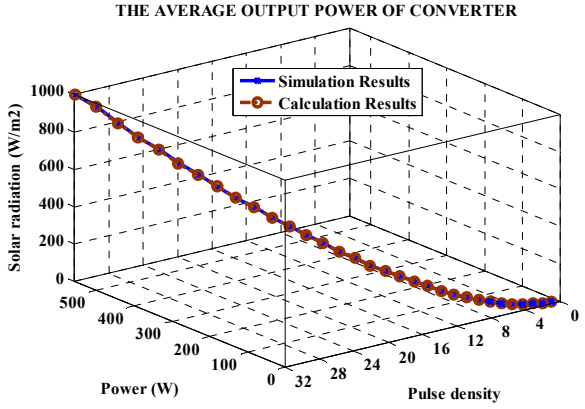

Fig. 10. The average output power of converter according to the pulse density and solar radiation variations

To test the proposed system, solar radiation level is changed rapidly step by step as 250-500-750 and 1000 W/m^2 in PSIM program and P&O MPPT algorithm is examined. The theoretical PV power (P_{ref}) and the obtained PV power (P_{pv}) from the proposed system are shown in Figure 11.

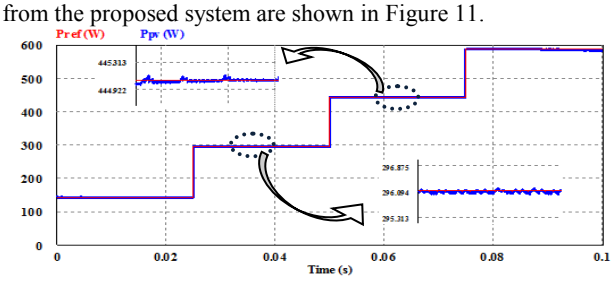

Fig. 11. P&O MPPT algorithm results

Figure 12 shows the ZCS condition while the system is tracking the MPP by PDM.

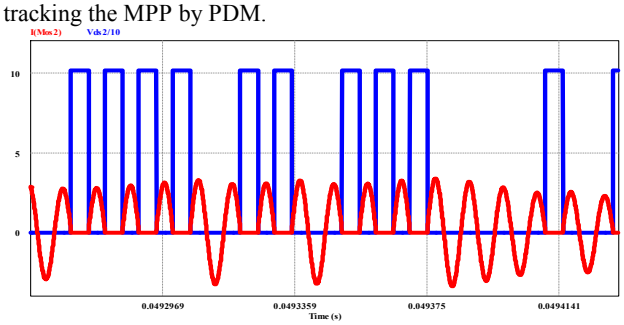

Fig. 12. ZCS condition

5. Conclusions

In this study, the proposed 32 PDM controlled full bridge series resonant converter obtained by using P&O MPPT algorithm is simulated at PSIM. The required power for MPPT algorithm is controlled by deleting some control pulses of series resonant converter operating at resonant frequency. Therefore, the output power is controlled at wide range with 100 kHz resonant frequency depending on the deleted control pulses and ZCS is provided continuously. The changes in the proposed 32 PDM patterns occurring depending on the power values obtained from PV panels and therefore the average output power changes of the series resonant converter are also examined. Validity of the PDM controlled MPPT converter is tested in 600 W PV generation system and soft switching conditions at 100 kHz are presented from 250 to 1000 W/m^2 radiation levels.

6. Acknowledgment

This research was supported by Karabuk University Research Projects Fund (No: KBU-BAP-15/2-DR-005). The authors would like to thank for support.

7. References

[1] O. Deveci, and C. Kasnakoglu, "Performance improvement of a photovoltaic system using a controller redesign based on numerical modeling" *International Journal of Hydrogen Energy*, vol. *41*, no. *29*, pp. *12634-12649*, Aug. 2016.

[2] M. A. Enany, M. A. Farahat, and A. Nasr, "Modeling and evaluation of main maximum power point tracking algorithms for photovoltaics systems", *Renewable and Sustainable Energy Reviews*, vol. *58*, pp. *1578-1586*, Feb. 2016.

[3] S. Borekci, E. Kandemir, and A. Kircay, "A simpler single-phase single-stage grid-connected PV system with maximum power point tracking controller", *Elektronika Ir Elektrotechnika*, vol. *21*, no. *4*, pp. *44-49*, Apr. 2015.

[4] H. Fujita, and H. Akagi, "Pulse-density-modulated power control of a 4 kW, 450 kHz voltage-source inverter for induction melting applications", *IEEE Trans. on Industry Applications*, vol. *32*, no. *2*, pp. *279-286*, Mar./Apr. 1996.

[5] R. L. Steigerwald, R. W. De Doncker, and M. H. Kheraluwala, "A comparison of high-power DC-DC soft-switched converter topologies", *IEEE Trans. on Industry Applications*, vol. *32*, no. *5*, pp. *1139-1145*, Sep./Oct. 1996.

[6] B. Nagarajan, and R. R. Sathi, "Phase locked loop based pulse density modulation scheme for the power control of induction heating applications", *Journal of Power Electronics*, vol. *15*, no. *1*, pp. *65-77*, Jan. 2015.

[7] S. Oncu, and S. Nacar, "Soft switching maximum power point tracker with resonant switch in PV system", *International Journal of Hydrogen Energy*, vol. *41*, no. *29*, pp. *12477-12484*, Aug. 2016.

[8] M. K. Kazimierczuk, and D. Czarkowski, "Resonant Power Converters", John Wiley & Sons Inc, Chap. 19, 1995.

[9] S. Tian, F. C. Lee, and Q. Li, "A simplified equivalent circuit model of series resonant converter", *IEEE Trans. Power Electronics*, vol. *31*, no. *5*, pp. *3922-3931*, 2016.

[10] S. Oncu, and H. Ozbay, "Simulink model of parallel resonant inverter with DSP based PLL controller", *Elektronika Ir Elektrotechnika*, vol. *21*, no. *6*, pp. *14-17*, Sep. 2015.

[11] M. Z. Zainol, N. A. Rahim, and J. Selvaraj, "Design and analysis of contactless transformer using series resonant converter", *Przegląd Elektrotechniczny*, vol. *89*, no. *5*, pp. *192-195*, 2013.

[12] M. Mohammadi, and M. Ordonez, "Fast transient response of series resonant converters using average geometric control", *IEEE Trans. Power Electronics*, vol. *31*, no. *9*, pp. *6738-6755*, Sep. 2016.

[13] V. Esteve et al., "Improving the efficiency of IGBT series-resonant inverters using pulse density modulation", *IEEE Trans. Industrial Electronics*, vol. *58*, no. *3*, pp. *979-987*, Mar. 2011.

[14] S. Oncu, and A. Karafil, "Pulse density modulation controlled converter for PV systems", *International Journal of Hydrogen Energy*, vol. *42*, no. *28*, pp. *17823-17830*, 2017.

[15] J. Essadaoui, P. Sicard, E. Ngandui, and A. Cheriti, "Power inverter control for induction heating by pulse density modulation with improved power factor", in *Proc. IEEE Canadian Conference on Electrical and Computer Engineering (CCECE)*, 2003, pp. *515-520*.

[16] P. Kowstubha, K. Krishnaveni, and K. R. Reddy, "Review on different control strategies of LLC series resonant converters", in *Proc. IEEE Int. Conf. Advances in Electrical Engineering (ICAEE)*, 2014, pp. *1-4*.

[17] M. A. Eltawil, and Z. Zhao, "MPPT techniques for photovoltaic applications", *Renewable and Sustainable Energy Reviews*, vol. *25*, pp. *793-813*, May 2013.